Supplement of Hydrol. Earth Syst. Sci., 28, 1173–1190, 2024
https://doi.org/10.5194/hess-28-1173-2024-supplement

Hydrology and Earth System Sciences
Open Access
EGU

Supplement of

Check dam impact on sediment loads: example of the Guerbe River in the Swiss Alps – a catchment scale experiment

Ariel Henrique do Prado et al.

Correspondence to: Ariel Henrique do Prado (ariel.doprado@geo.unibe.ch)

S1. Supplementary figures and tables

Here we illustrate an example of a digital surface model (DSM) and an orthomosaic image (Figs. S1) from the analyzed gravel bars, which we retrieved using the structure from motion photogrammetric processing of our UAV-derived images (Table S1). We provide an example of how we employed the Wolman grid approach to the orthomosaic images for conducting grain size measurements (Fig. S1). This is followed by an example where we show how the grain sizes were manually measured using the QGIS software (Fig. S2). The engineered slopes for all check dams in the Guerbe River are shown in the plot of Fig. S3. These slopes here were calculated using the LIDAR DEM SwissALTI3D from 2019 as a basis. The water discharge data, which has been recorded at the Burgistein gauging station, considers the period between 2009 and 2021; it is shown in Fig. S4. We also display aerial images taken between 1977 and 2021 (Figs. S5) from the Riselbruch, which is a hillslope in the knickpoint zone (see Fig. 2 of the main text). These images show the landslide activity in the region before and after the construction of the check dams.

Table S2 compiles the data as grain size percentiles and the slopes with a 95% confidence interval. This table also contains the coordinates in the WGS format together with the number of measured grains and information on the channel widths of each surveyed site. Table S3 shows the gamma distribution parameters fitted for the grain size percentiles. This was calculated using the method proposed by Mair et al. (2022, see reference in the main text) to propagate the errors related to the photogrammetric methods (see section 3.3.5 in the main text). Finally, in Table S4 we illustrate the results where we reconstruct the armour-breaking occurrence during the peak discharge in 2021. This is calculated for each surveyed site considering engineered and non-engineered states using the MP.M. and Reacking equations as a basis. We considered that the amour would be broken if the shear stress is large enough so that the D_{84} in riverbed can be entrained. We thus considered this to occur if the calculated bedload flux was larger than 0.001 m^3 s^{-1} during the 2021 peak discharge.

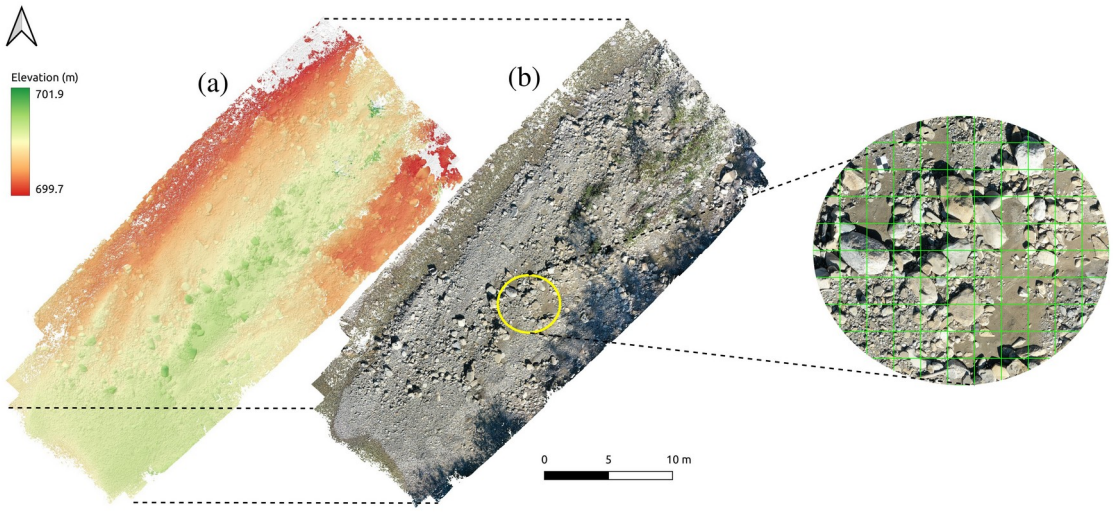

Figure S1. Examples of (a) a Digital Surface Model (DSM) and (b) an orthomosaic resulting from the photogrammetry processing. In the circle, there is an example of a Wolman grid with a spacing of 0.5 meters. The data were acquired in the Guerbe River (Site 9 in the main text) in 2021.

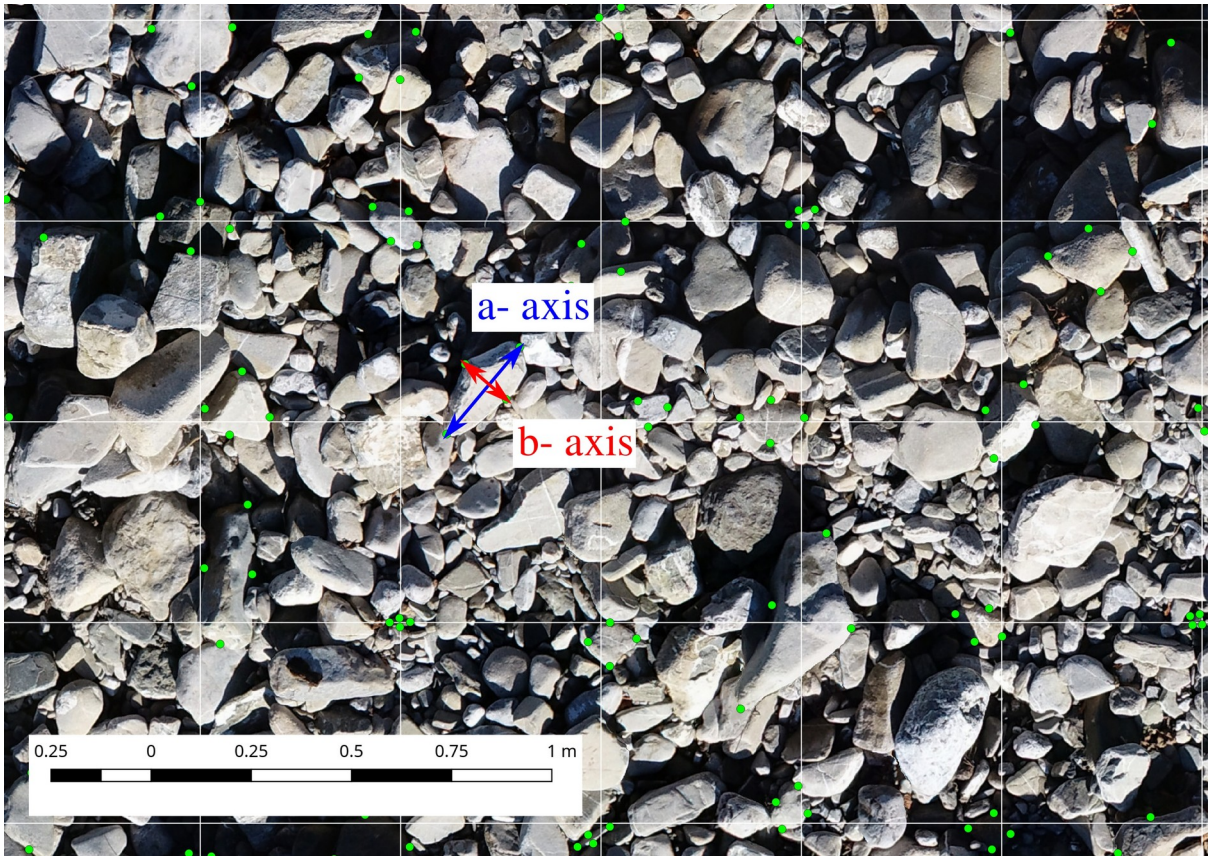

Figure S2. Example of how we measured the lengths of the a- and b- axes using the Qgis software.

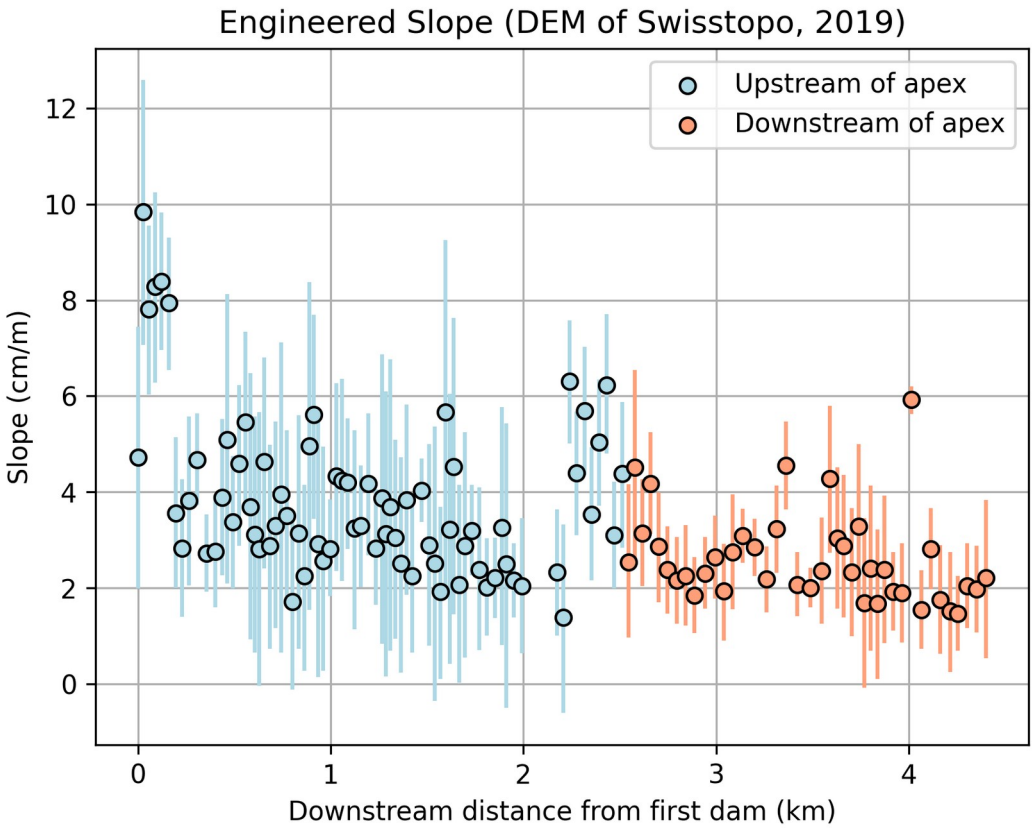

Figure S3. The engineered slopes of gravel bars between all check dams in the Guerbe River along with the 95% confidence interval (vertical lines). The slopes were measured using the 0.5 m grid resolution LiDAR DEM SwissALTI3D (Swisstopo, 2019) as a basis. The uncertainty in elevation for this DEM is 0.5 m.

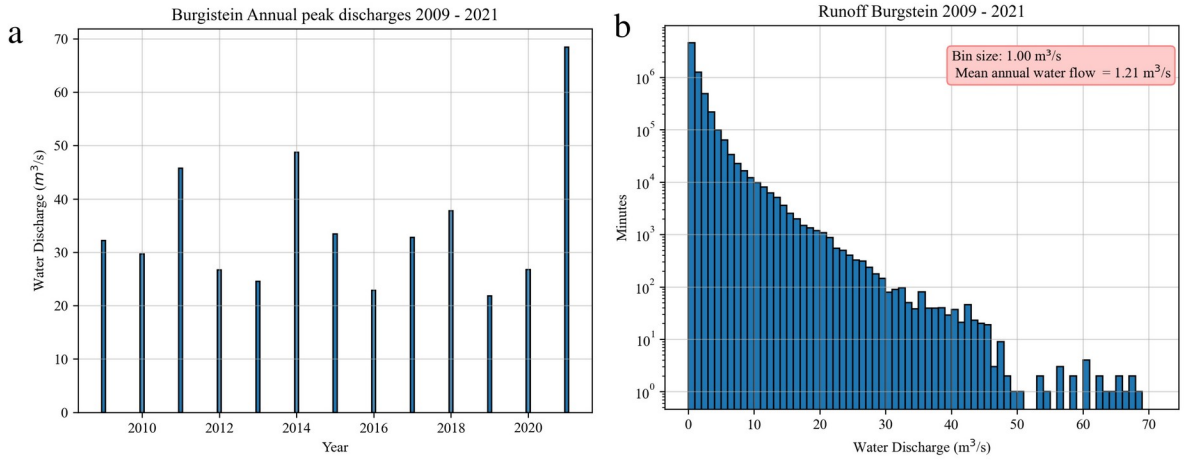

Figure S4. Discharge values measured at the Burgistein gauging station for the Guerbe River. (a) Values of annual peak discharge for the period between 2009 and 2021. (b) Histogram with the discharge values (m^3/s) that were measured every minute during the same period.

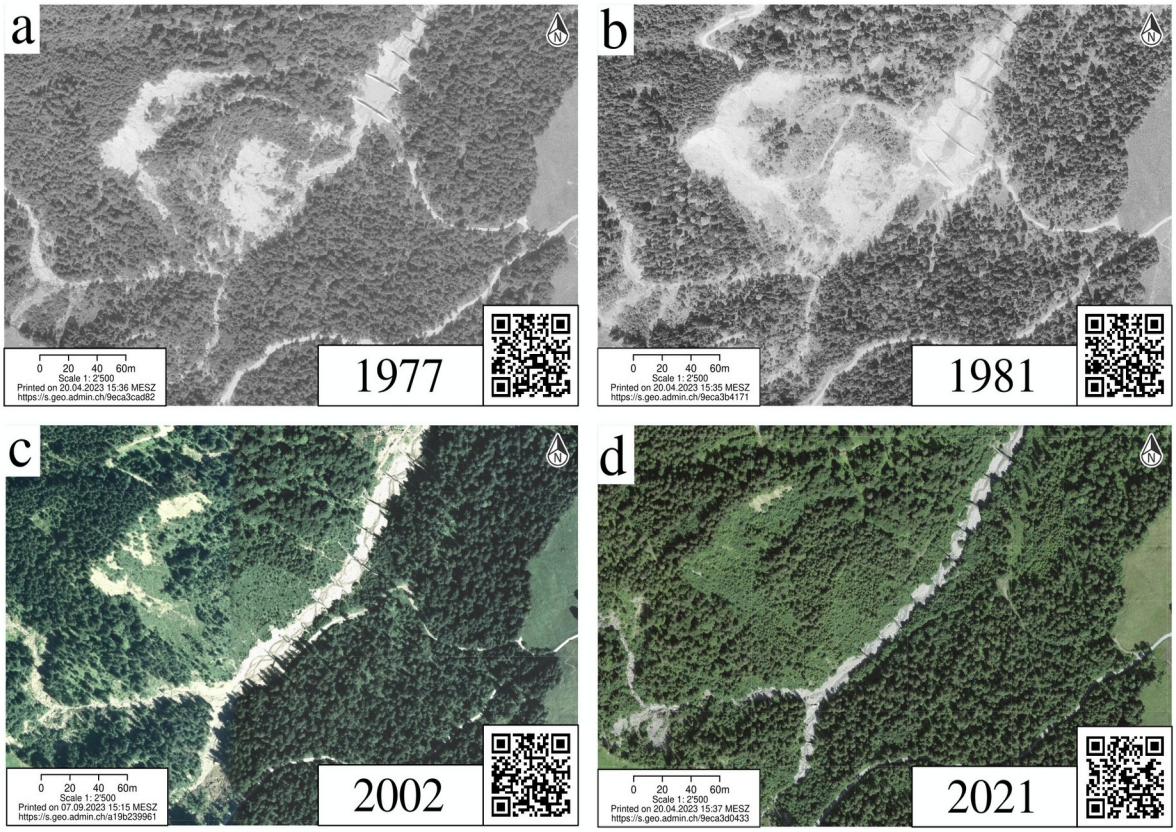

Figure S5. Temporal evolution of the Guerbe River over the last five decades at the Riselbruch (Knickpoint zone indicated in the circle in Fig. 2 in the main text). (a) The aerial image taken in 1977 shows that a large landslide situated upstream of the uppermost constructed check dam (on the northern side of the river) was active. (b) In 1981, new check dams were under construction in this upstream area. (c) and (d) Aerial images taken in 2002 and 2021 reveal that the landslide observed in (a) and (b) has stabilized after the construction of the new check dams, leading to a gradual reforestation of the surrounding area. Copyright, Swiss federal authorities. http://www.disclaimer.admin.ch/terms_and_conditions.html. © CNES, Spot Image, swisstopo, NPOC.

Table S1: Summary of the UAV surveys and resulting SfM model uncertainties. RMSE = root mean square error, Std = standard deviation, px = pixel.

Survey (Site)	1	2	3	4	5	6	7	8	9	10	11	12	13
Flight height nominal (m)	7.11	5.02	6.7	8.36	6.04	7.31	7.91	6.8	7	6.32	6.98	7.42	6.58
Ground sampling distance (mm)	1.5	1.47	1.42	1.83	1.41	1.6	1.7	1.45	1.5	1.37	1.52	1.59	1.63
Number of images used	35	43	46	142	91	130	269	190	212	141	87	87	180
Image acquisition format	JPEG	JPEG	JPEG	JPEG	JPEG	JPEG	JPEG	JPEG	JPEG	JPEG	JPEG	JPEG	JPEG
Number of used GCPs	10	10	5	8	8	10	10	10	10	10	10	8	8
Control Point RMSE (mm)													
X, Y	29	73.8	78.6	26.4	23.70	16.52	18.77	15.39	9.81	10.48	13.34	18.11	11.95
Z	13.5	31.7	37.1	10.5	9.37	19.27	28.20	11.74	13.33	6.06	7.42	25.76	41.96
Check Point RMSE (mm)													
X, Y	39.9	80.6	-	22.2	30.27	21.64	15.36	17.59	23.64	17.11	13.38	23.46	15.20
Z	36.3	52.3	-	1.5	57.03	28.95	41.67	8.22	18.07	17.83	18.43	30.03	52.96
Tie Point Observation Distance (m)													
Mean	7.2	4.65	6.28	8.29	5.94	7.21	7.23	6.28	6.49	5.83	6.48	6.87	5.98
Std	0.4	0.4	0.55	0.35	0.38	0.44	0.45	0.43	0.36	0.41	0.23	0.25	0.15
Sparse point cloud precision (mm)													
Mean Z	14.2	10.0	10.8	8.2	4.50	3.88	14.23	5.59	5.04	7.52	6.61	4.37	4.79
Std Z	14.1	5.9	10.5	7.4	3.71	3.0	10.96	7.23	4.28	6.64	5.80	3.71	10.96
Image error (px)	1.7	4.3	1.39	0.66	1.02	0.82	1.74	0.77	0.81	1.21	0.98	0.72	0.57
Reprojection error RMSE (px)	1	1.16	1.52	0.54	0.57	0.64	1.04	0.85	0.68	0.73	0.74	0.63	0.90
Doming amplitude (m)	0.08	-0.08	0.16	-0.06	0.051	-0.009	0.081	-0.032	0.019	-0.011	-0.018	-0.035	0.008
Orthophoto mosaic resolution (mm px^{-1})	2.84	2.29	2.74	3.67	2.81	3.2	3.41	2.89	3	2.73	3.04	3.19	3.26

Table S2. Grain sizes and slopes of Guerbe River bars along the engineered reach with the presence of the check dams (Map in Fig.1 of the main text).

Site	Coordinates latitude (DD WGS 84)	Coordinates longitude (DD WGS 84)	Number of grains	D50 (cm)	D50 95% C.I. (cm)	D84 (cm)	D84 95% C.I. (cm)	Eng. Slope (m/m)	Eng. Slope 95% C.I. (m/m)	Non-eng. Slope (m/m)	Non-eng. Slope 95 % C.I. (m/m)	Channel Width (m)
1	7.4709	46.7297	475	8.13	7.06 - 9.38	26.73	23.58 - 30.02	9.7	8.6 - 11.0	-	-	16.4
2	7.4738	46.7321	458	6.36	5.80 - 6.89	16.47	14.39 - 18.94	4.9	4.5 - 5.2	22.5	22.3 - 22.7	15.7
3	7.4773	46.734	811	5.44	5.10 - 5.78	11.10	10.36 - 11.85	3.3	3.0 - 3.7	25.8	25.6 - 26.0	13.7
4	7.488	46.7399	696	7.38	6.72 - 8.00	18.54	16.51 - 21.49	2.2	2.2 - 2.4	7.81	7.74 - 7.92	16.0
5	7.4891	46.7405	675	6.08	5.54 - 6.74	15.64	13.81 - 17.63	2.7	2.5 - 2.9	16.6	16.4 - 16.6	16.4
6	7.4914	46.741	1145	4.20	3.95 - 4.46	12.63	11.06 - 14.65	2.7	2.2 - 3.2	19.0	18.7 - 19.3	19.9
7	7.4987	46.7428	1450	4.29	4.04 - 4.56	16.48	14.76 - 18.08	0.039	0.037 - 0.040	0.105	0.101 - 0.107	23.63
8	7.5018	46.7432	1170	4.49	4.26 - 4.75	10.27	9.56 - 10.98	0.031	0.030 - 0.034	0.086	0.084 - 0.088	17.43
9	7.509	46.7456	1419	4.92	4.63 - 5.24	17.84	16.51 - 19.44	0.021	0.018 - 0.027	0.070	0.069 - 0.070	15.01
10	7.5133	46.748	738	4.89	4.42 - 5.45	17.04	15.49 - 19.09	0.031	0.030 - 0.032	0.062	0.060 - 0.064	15.22
11	7.516	46.7508	371	4.48	3.99 - 5.17	14.87	12.94 - 17.02	0.013	0.012 - 0.014	0.054	0.054 - 0.055	15.84
12	7.5164	46.7512	494	3.67	3.36 - 4.00	8.64	7.85 - 9.68	0.020	0.018- 0.021	0.059	0.057 - 0.060	18.16
13	7.5191	46.7553	1427	3.32	3.15 - 3.52	9.34	8.76 - 9.92	0.015	0.013 - 0.017	-	-	20.0

Table S3. Gamma probability density function (PDFs) parameters for the uncertainty estimation using a combined bootstrapping and Monte Carlo error modelling for the grain size percentile values (D_{50} and D_{84}).

Site	D_{50} Gamma A	D_{50} Gamma Loc	D_{50} Gamma Scale	D_{84} Gamma A	D_{84} Gamma Loc	D_{84} Gamma Scale
1	51.4	38.2	0.86	83.8	109	1.92
2	856	-17.5	0.0947	43.6	93	1.65
3	1850	-21.3	0.0409	759	3.97	0.141
4	1470	-52.2	0.0859	13.8	138	3.54
5	51.3	38.4	0.441	131	49.2	0.82
6	404	16.2	0.064	25.4	79.4	1.86
7	145	26.1	0.116	399	-12.7	0.443
8	33100	-173	0.00658	131	60.5	0.323
9	131	31.8	0.133	65.2	117	0.955
10	54.9	29.4	0.356	445	-31.9	0.458
11	21.1	30.9	0.675	27.1	94.1	2.04
12	86.9	21	0.181	25.3	64.4	0.882
13	163	21.1	0.0755	1430	-16.6	0.077

Table S4. Armour break occurrences during the peak discharge of 2021 for each surveyed site considering engineered and non-engineered scenarios and using the MP.M. and Reacking equations as a basis. We considered that the amours will break if the shear stress is large enough so that the D_{84} in riverbed can be entrained. Therefore, we considered such conditions if the calculated bedload flux is larger than 0.001 $m^3 s^{-1}$.

Site	Engineered MP.M.	Engineered Recking	Non-engineered MP.M.	Non-engineered Recking
1	No	No	No	No
2	No	No	Yes	Yes
3	No	Yes	Yes	Yes
4	No	No	Yes	Yes
5	No	Yes	Yes	Yes
6	No	Yes	Yes	Yes
7	No	Yes	Yes	Yes
8	Yes	Yes	No	Yes
9	No	No	Yes	Yes
10	No	Yes	Yes	Yes
11	No	No	Yes	Yes
12	Yes	Yes	Yes	Yes
13	No	Yes	No	Yes

S2. Workflow for the propagation of uncertainties upon estimating the bedload flux

The workflow for propagating the uncertainty comprises an estimation of the uncertainties of the initial parameters and an assessment of the uncertainty related to the bedload fluxes. Each parameter (grain size, channel slope, and width) follows a specific workflow:

- **Grain Sizes**:
  - We employed the method developed by Mair et al. (2022) for estimating the uncertainties related to the measurements of grain sizes, utilizing survey-specific Structure-from-Motion (SfM) uncertainties (Table S1). This involved a routine combining bootstrapping and Monte Carlo simulation, which was conducted separately for each river bar.
  - In each bootstrap scenario (n = 1000), we resampled all measured grains, simulating distortions related to the survey-specific SfM for each grain (details in Mair et al., 2022). Uppon bootstrapping, the D_{50} and D_{84} were stored for each scenario.
  - After the bootstrap, we fitted all stored D_{50} and D_{84} values into a gamma distribution for a subsequent simulation and calculation of bedload fluxes through the Monte Carlo simulation framework. We justify the use of the gamma distribution due to the non-normality of the D_{50} and D_{84} distributions. The median, as well as the 95% confidence interval, were calculated for D_{50} and D84s.
- **Slope**:
  - Slope uncertainties were calculated by applying a bootstrap (n = 1000) on the data that we collected at each surveyed site. For each scenario, the median slope was stored.
  - After the bootstrap, we calculated the 95% confidence interval and fitted a normal distribution to the slope values.
- **Widths**:
  - The uncertainties on the channel width data were estimated by assuming that the values are uniformly distributed. Here, we considered the range of measured widths at each side, and we assigned an uncertainty of ±10% to these values.

Bedload Flux Uncertainties:

- The uncertainties related to the bedload flux was determined using a Monte Carlo simulation (n = 1000), where each scenario calculated the bedload flux using input parameters sampled from random variables (rsv function in Python). Here, we used the distribution of values that we estimated in the previous steps as a basis.
- The confidence intervals of the calculated bedload fluxes were then determined from these scenarios.